Deficient Hippocampal Long-Term Potentiation in α-Calcium-Calmodulin Kinase II Mutant Mice

Alcino J. Silva; Charles F. Stevens; Susumu Tonegawa; Yanyan Wang

Science, New Series, Vol. 257, No. 5067 (Jul. 10, 1992), 201-206.

Stable URL:
http://links.jstor.org/sici?sici=0036-8075%2819920710%293%3A257%3A5067%3C201%3ADHLPIK%3E2.0.CO%3B2-E

Science is currently published by American Association for the Advancement of Science.

---

17. Cas and Wright (*8*) suggested that intracaldera tuffs do not result from pyroclastic flow and hence are not true pyroclastic flow deposits. They do not explain the processes they envision, but in this situation pyroclastic emplacement without some form of lateral flow is clearly impossible, even in near-vent locations.
18. M. J. Branney and R. S. J. Sparks, *J. Geol. Soc. London* **147**, 919 (1990).
19. For example, halloysite, smectites, sericite, montmorillonite, kaolinite, and illite.
20. R. L. Allen, *Econ. Geol.* **83**, 1424 (1988).
21. P. W. Lipman, *Geol. Soc. Am. Bull.* **87**, 1397 (1976).
22. L. Draper, *Marine Geol.* **5**, 133 (1966); P. D. Komar, *J. Sed. Petrol.* **44**, 169 (1974); B. Butnam *et al.*, *J. Geophys. Res.* **84**, 1182 (1979).
23. See K. T. Pickering *et al.*, *Deep Marine Environments* (Unwin Hyman, London, 1989).
24. R. S. J. Sparks, *Bull. Volcanol.* **48**, 3 (1986).
25. K. V. Cashman and R. S. Fiske, *Science* **253**, 275 (1991). These authors described a fallout deposit resting above a coeval hot-emplaced (~450°C) flow deposit, which we suggest is most likely to have formed from the material that would not be incorporated into the convective column above the vent.
26. P. Kokelaar, *Bull. Volcanol.* **48**, 275 (1986), figure 4. A bell-shaped exclusion zone postulated to occur above the vent was referred to in that case as a "cupola of steam," because the explosivity involves bulk incorporation of water in the eruptive conduit, so that the gas of the erupted dispersion is dominated by (nonmagmatic) steam; see P. Kokelaar, *J. Geol. Soc. London* **140**, 939 (1983).
27. P. D. Rowley *et al.*, *U.S. Geol. Surv. Prof. Pap. 1250* (1981), p. 489.
28. Compare with R. S. Fiske and T. Matsuda, *Am. J. Sci.* **262**, 76 (1964).
29. H. Ohmoto and B. J. Skinner, *Econ. Geol. Monogr.* **5**, 1 (1983).
30. P. Kokelaar, *Geol. Soc. Am. Bull.*, in press.
31. C. J. Busby-Spera and J. Saleeby, *Geologic Guide to the Mineral King Area, Sequoia National Park, California* (Society of Economic Paleontologists and Mineralogists, Los Angeles, 1987).
32. T. G. Gloppen and R. J. Steel, *Soc. Econ. Paleontol. Mineral. Spec. Publ.* **31**, 49 (1981).
33. Supported by a NATO collaborative research grant 910549 and NSF grant EAR9018606 (to C.B.). We are grateful to G. Lloyd for assistance with production of the SEM image and to M. J. Branney, R. V. Fisher, S. Self, and R. S. J. Sparks for reviews of a draft of the article.

RESEARCH ARTICLES

Deficient Hippocampal Long-Term Potentiation in α-Calcium-Calmodulin Kinase II Mutant Mice

Alcino J. Silva, Charles F. Stevens, Susumu Tonegawa, Yanyan Wang

As a first step in a program to use genetically altered mice in the study of memory mechanisms, mutant mice were produced that do not express the α-calcium-calmodulin–dependent kinase II (α-CaMKII). The α-CaMKII is highly enriched in postsynaptic densities of hippocampus and neocortex and may be involved in the regulation of long-term potentiation (LTP). Such mutant mice exhibited mostly normal behaviors and presented no obvious neuroanatomical defects. Whole cell recordings reveal that postsynaptic mechanisms, including *N*-methyl-D-aspartate (NMDA) receptor function, are intact. Despite normal postsynaptic mechanisms, these mice are deficient in their ability to produce LTP and are therefore a suitable model for studying the relation between LTP and learning processes.

Long-term potentiation (LTP) is an electrophysiological manifestation of a long-lasting increase in the strength of synapses that have been used appropriately (*1*). Although LTP has been studied as a mechanism responsible for some types of learning and memory, the actual evidence for this hypothesis is not extensive. The main support for LTP as a memory mechanism is the observation that pharmacological agents that block hippocampal glutamate receptors of the *N*-methyl-D-aspartate (NMDA) class and thus prevent the induction of LTP also impair spatial learning in rodents (*2*). The problem with this evidence is that blocking NMDA receptors disrupts synaptic function and thus potentially interferes with the in vivo computational ability of hippocampal circuits. Perhaps the failure of learning results not from the deficit in LTP but simply from some other incorrect operation of hippocampal circuits that lack NMDA receptor function.

We have adopted a strategy for the study of the mechanisms of mammalian memory, designed to address the relation of LTP to learning; we have produced mice with mutations in individual enzymes likely to be involved in the regulation of candidate memory mechanisms, such as LTP. These specific mutations were made with the use of gene targeting (*3*). As a first step in this program, we report studies on a strain of mutant mice that do not express the α isoform of calcium-calmodulin–dependent protein kinase type II (α-CaMKII). This enzyme is neural-specific and is present presynaptically and appears abundantly adjacent to the postsynaptic membrane at synapses that express LTP (*4*, *5*). Calmodulin (CaM) loaded with calcium (Ca^{2+}) activates this enzyme and induces its autophosphorylation. Once autophosphorylated, the CaMKII holoenzyme no longer requires Ca^{2+} or CaM for activity. This switch-like mechanism can maintain the enzyme in an active state beyond the duration of the activating Ca^{2+} signal (*6*) and has been invoked in learning models (*7*). Pharmacological experiments have implicated this holoenzyme in the induction of LTP (*8*, *9*). Although postsynaptic mechanisms seem normal in the CA1 hippocampal region of these mutant mice, we find little or no LTP. We thus have a strain of mice that should be suitable for studying the behavior implications of normal synaptic transmission but deficient LTP. In the accompanying paper we show that these mutant mice are impaired in performing a spatial-learning task (*10*).

α-CaMKII mutant mice. In order to produce mice with a mutation in the α-CaMKII locus, we constructed the plasmid p23 (Fig. 1A) which contains a 6.1 kilobase (kb) mouse genomic α-CaMKII sequence that is disrupted by insertion of a neomycin-resistance gene (*neo*) from the plasmid *pgk-neo* (*11*). The insertion is within the α-CaMKII exon encoding most of the regulatory domain, and the inserted sequence replaced a 130-bp mouse genomic sequence flanked by a pair of Sph I sites; the expression product of the 130-bp sequence includes the entire inhibitory domain and five amino acids in the amino end of the calmodulin-binding domain (*12*). We transfected the linealized (Fig. 1A) p23 plasmid into E14 embryonic stem (ES) cells (*13*) by electroporation (*13*) and isolated 150 (*neo*) colonies, of which two (E14-20 and E14-84) were shown by Southern blotting analysis to harbor a homologously integrated plasmid.

We injected the E14-20 ES cells into C57B1/6J blastocysts and transferred the blastocysts into pseudo-pregnant mothers. Twelve male chimeric mice were born; they were bred with BALB/c females. Hybridization blot analysis (Southern) of tail DNA from the offspring of the chimeric males,

A. J. Silva and S. Tonegawa are at the Howard Hughes Medical Institute, Center for Cancer Research and Department of Biology, Massachusetts Institute of Technology, Cambridge, MA 02139. C. F. Stevens and Y. Wang are at the Howard Hughes Medical Institute, Salk Institute, 10010 North Torrey Pines Road, La Jolla, CA 92037.

revealed that 11 of the 12 males transmitted the α-CaMKII mutation to 20 to 40 percent of their offspring. Southern blot analysis of a litter from a cross between two mice heterozygous for the α-CaMKII mutation identified mice with two mutant copies of the α-CaMKII locus (mutation homozygous), as well as mice with one mutant copy (mutation heterozygous) and mice with normal α-CaMKII loci (wild type) (Fig. 1B). After multiple crosses of this type, the genotype distribution among the total progeny was close to 1:2:1 for wild-type, mutation-heterozygous, and mutation-homozygous mice, a ratio expected for the segregation of a nonlethal mutation. Since we have homozygous mice that were born in June 1990, the α-CaMKII mutation appears not to affect long-term survival under laboratory conditions. In the experiments described below, unless otherwise noted, we used as controls the wild-type littermates of the mutant mice.

Northern (RNA) blot analysis of total brain RNA confirmed that the α-CaMKII mutant mice lacked α-CaMKII mRNA, or any truncated form of it, whereas the β-CaMKII mRNA was normal. Immunoblot analysis of forebrain tissue from the mutants and their normal littermates with the monoclonal antibody 6J9 (5), which recognizes the α-CaMKII, confirmed the absence of α-CaMKII in the mutants but the presence in the mutation- heterozygous and the wild-type mice (Fig. 1C). Using a similar analysis with a polyclonal antibody that recognized β-CaMKII, we detected the kinase in all three types of mice (Fig. 1C). Consistent with the complete absence of α-CaMKII in the mutant mice is the decrease (45 ± 4 percent) of in vitro phosphorylation of a CaMKII-specific peptide substrate, synthide 2, by the homogenates of the forebrains of these mice as compared to that of the control mice (*14*). In contrast, such difference in the in vitro phosphoryla-

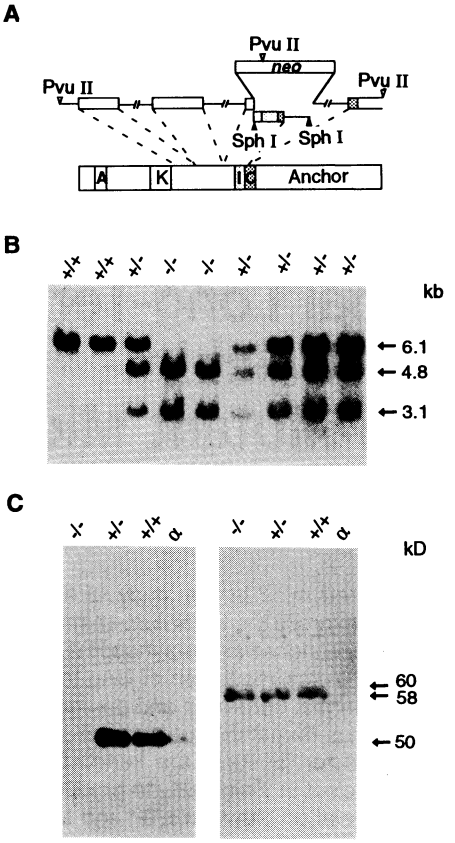

Fig. 1. Lack of α-CaMKII in the α-CaMKII mutant mice. (**A**) Schematic representation of the p23 construct used for the targeting experiment. The 6.1-kb Pvu II genomic fragment used in the construction of p23 (*27*), as well as the *neo* and its insertion site are shown on the upper part. The deleted Sph I fragment and the functional domains of the α-CaMKII enzyme are shown in the lower tracings. The intron-exon boundaries and their correspondence to the functional domains of the protein are shown by the dashed lines. (**B**) Southern analysis of the DNA isolated from tails of 5-week old offspring from a cross of α-CaMKII mutation heterozygous (*28*). The genotypes of the offspring are shown above the autoradiographs. (**C**) Immunoblot (Western) analysis with a monoclonal antibody (6g9) that recognizes α-CaMKII (left), and with a polyclonal antibody that recognizes the β-CaMKII, and β′-CaMKII ("Darcy"; right) of forebrain homogenates (5 mg) from a mutation homozygous, mutation heterozygote and wild type (see notation above autoradiographs). As a control, purified rat α-CaMKII protein (70 ng) was included next to the other samples in the immunoblot procedure. Parallel to the autoradiographs, we show the molecular mass of the protein bands detected [α-CaMKII, β-CaMKII and β′-CaMKII respectively, 50, 58, and 60 kD (*29*)]. A, ATP binding domain; K, catalytic domain; I, inhibitory domain; C, CaM binding domain; Anchor, association-anchor domain; −/−, mutant homozygous; +/−, mutant heterozygous; +/+, wild type.

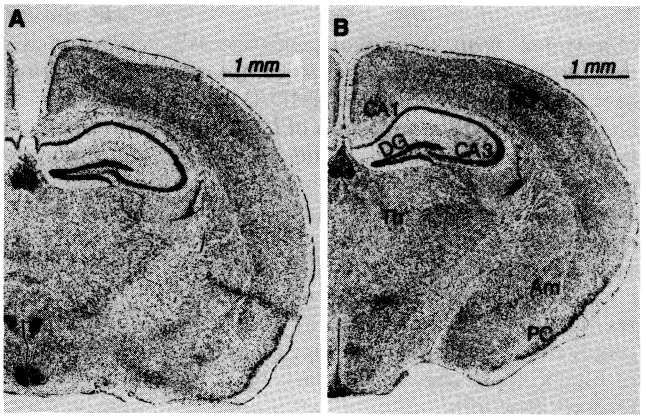

Fig. 2. Coronal sections from a wild-type (**A**) and α-CaMKII mutant (**B**) mouse brain. The frozen brain sections (14 μm) were thaw-mounted on slides coated with gelatin and stained with 1 percent thionin. The rostral-caudal level of the two slices were matched for the hippocampus, but because of slightly different angles of sectioning, the ventral portion of the slice from the α CaMKII mutant mouse is posterior to the one from the wild-type mouse. Am, amygdala; CA1 and CA3, pyramidal cell fields of the hippocampus; DG, dentate gyrus; NC, neocortex; PC, pyriform cortex; Th, thalamus.

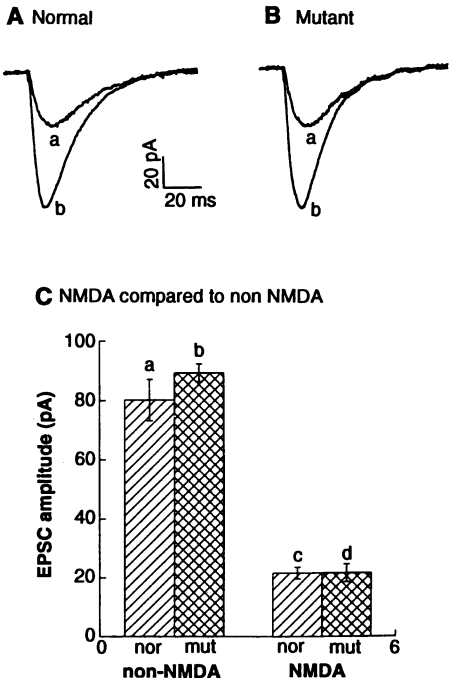

Fig. 3. Synaptic currents from whole cell recordings as a function of time for normal (**A**) and mutant (**B**) mice. The superimposed pair of traces in (A) and (B) show the total synaptic current that includes both the NMDA and non-NMDA components (b) and the NMDA component alone (a). The NMDA component was obtained by subtracting the non-NMDA component remaining after application of 50 μM D-APV (an antagonist of NMDA receptor; traces not shown) from the total current (b). The averages of EPSC amplitudes for non-NMDA and NMDA components from eight normal (nor) and eight mutant (mut) mice are shown in the histogram (**C**). The holding potential was −50 mV, and the stimulus intensity was increased to reveal the NMDA (in addition to non-NMDA) components of the synaptic currents. The NMDA components were measured at 20 to 35 ms after the peak current (always judged by the traces mostly after D-APV or at −80 mV). There is no significant difference between a and b ($P > 0.2$, t test), and between c and d ($P > 0.9$).

tion levels was not observed with the homogenates of cerebellum, where the α isoform is known to be a minor CaMKII component (*5*, *15*). We confirmed the specificity of our CaMKII assays by adding a peptide inhibitor of CaMKII activity (*16*) and showing that it reduces phosphorylation levels by 95 percent.

Ca^{2+}-calmodulin–independent kinase II activity of the forebrain of mutant mice was also measured and shown not to be increased compared to control mice (n = 4). This observation, as well as the lack of any truncated RNA (see above), suggests that the mutant mice do not harbor truncated α-CaMKII enzyme, which retains the catalytic domain without the inhibitory domain.

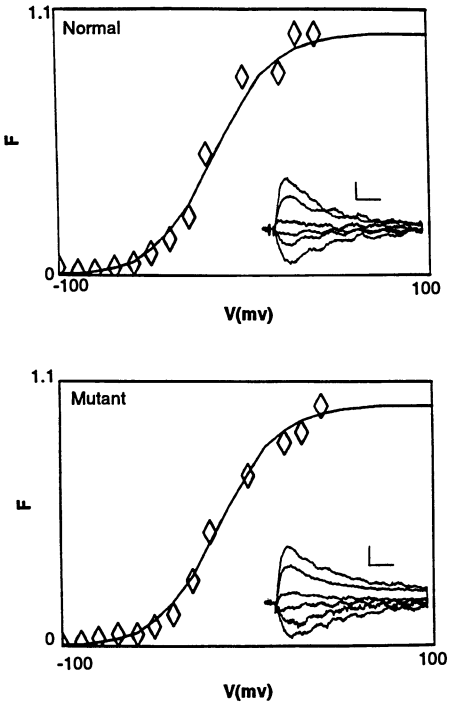

Fig. 4. Voltage dependence of NMDA receptor channels for typical normal (top) and mutant (bottom) neurons in the presence of CNQX (10 μM) and PCTX (50 μM). The fraction (F) of the maximum conductance through the NMDA receptor channels is given as a function of membrane potential. The insets show sample traces of synaptic current as a function of times. The holding potentials (mV) for the sample traces are (from top to bottom) +40, +30, +20, −90, −30, −20 for normal neuron and +40, +30, +20, −70, −40, −20 for mutant neuron. The vertical calibration bars indicate 25-pA current. The horizontal bars indicate 10 and 15 ms for normal and mutant neurons, respectively. The smooth curves were fitted with the following equation:

$$g(V) = 1/[1 + \exp(-0.062V)(C/3.57)]$$

where g is conductance in picoseconds, V is membrane potential in millivolts, and C is the extracellular magnesium concentration (millimolar) (*20*). No free parameters were used in fitting the theoretical curve to the data.

Gross anatomy and behavior. The observations by light microscopy revealed no obvious differences between the mutants and wild-type mice. We concentrated our survey on the hippocampus and neocortex, two structures with the highest expression of α-CaMKII (*15*). A comparison between coronal brain sections, stained with thionin, from mutants and wild-type mice (n = 3) (Fig. 2) indicated that the arrangement of cells in the major layers of the neocortex and hippocampus appeared to be normal. Tangential sections of the somatosensory cortex, stained with cytochrome oxidase or with cresyl violet, revealed the same topographical organization of the barrel fields as described for normal mice.

The behavior of the mutant mice appeared normal. The mutant pups gained weight at the same rate as their normal littermates, which suggests that their suckling behavior was not deficient. The mutants whisk, sniff, and mate, and they are not ataxic, indicating that the absence of the α-CaMKII does not result in generalized loss of neuronal function. The mutant mice are, however, more jumpy than their wild-type littermates. For instance, unlike the wild-type littermates mutant mice try frantically to avoid human touch long after they were weaned. This "nervousness" has been reported for animals with hippocampal lesions (*17*). Silva *et al.* (*10*) showed that the mutant animals are deficient in the spatial version of the Morris task, a sensitive test of hippocampal function.

Synaptic function. Using whole cell recording in hippocampal slices, we have studied synaptic currents evoked in CA1 pyramidal cells by stimulating Schaeffer collaterals (*18*). Our conclusions are based on studies of 37 neurons or slices from 14 homozygotes and two slices from one heterozygote and 35 neurons or slices from 20 littermates or other strain.

Typical synaptic currents from mutant (M) and normal (N) hippocampal pyramidal neurons are illustrated in Fig. 3, A and B. These experiments were performed in normal magnesium (1.3 mM), and the neuron's membrane potential (−50 mV); that reveals the NMDA as well as the non-NMDA components of the synaptic currents. Although the absolute amplitude of the synaptic currents depended on stimulus intensity, we used comparable stimuli in all experiments and found no apparent difference in the peak size and time course of synaptic currents from normal and mutant mice. In the presence of 6-cyano-7-nitroquinoxaline-2,3-dione (CNQX) (10 μM; antagonist of non-NMDA receptor) and picrotoxin (PCTX) (50 μM; antagonist of $GABA_A$ receptor) and at holding potential −30 mV, the rise time of the NMDA component (average four to ten traces) was 6.1 ms (±0.5 SEM) for the normal mice (n = 4) and 6.1 ms (±0.4) for the mutant mice (n = 4); the decay time constant was

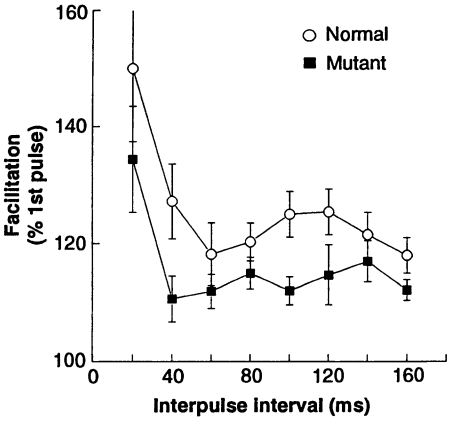

Fig. 5. Paired-pulse facilitation in normal and mutant mice. The size of the peak field potential for the second pulse of a pair (expressed as the percent of the first pulse size) as a function of the time interval between the pulses. Data are from ten normal and ten mutant slices. The error bars show the standard error of the mean (SEM).

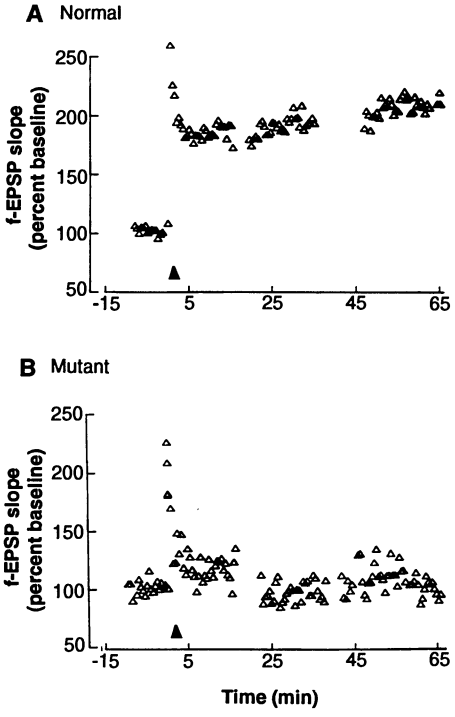

Fig. 6. Synaptic strength, expressed as a percentage of the average pre-tetanus initial field potential rate of change (f-EPSP), as a function of time in minutes during the experiments for a typical normal (**A**) and mutant (**B**) slice. Testing stimuli were given once each 30 s. Our standard tetanus, given at time = 0 (indicated by arrow head), was 100 Hz, three trains, and 20 pulses for each train with an intertrain interval of 11 s. In some mutant slices, a second tetanus (100 Hz, 200-ms duration, five trains, and 6-s interval) was given.

31.2 ms (±4.9) for the normal mice and 33.7 ms (±4.9) for the mutant mice. The rise time of the non-NMDA component (average 4 to 15 traces) was 1.5 ms (±0.2) for the normal mice (n = 4) and 1.6 ms (±0.1) for the mutant mice (n = 6); the decay time constant was 8.9 ms (±0.8) for the normal mice and 7.1 ms (±0.9) for the mutant mice at holding potential −80 mV. All above corresponding values were not significantly different (P values ranged from 0.2 to 0.9; t test). Furthermore, the ratio of NMDA to non-NMDA components did not differ between normal and mutant neurons (Fig. 3C): for eight normal neurons this ratio was 29.1 percent (±5), and for eight mutant neurons the ratio was 23.8 percent (±3; $P > 0.3$, t test).

The previous results showed that, at one particular voltage, the NMDA component of synaptic currents is the same size at normal and mutant synapses. The magnesium blocking of NMDA receptor channels, which endows these channels with the voltage dependence so important for making LTP associative, could differ between normal and mutant synapses. For example, the action of protein kinase C has been shown to modify the magnesium dissociate constant at the NMDA receptor regulatory site (*19*), and some direct or indirect action of α-CaMKII could possibly have an analogous effect. Were this the case, an essential difference in normal and mutant synaptic function would not have been revealed in the preceding experiments. Direct measurement of the voltage dependence of NMDA receptors in normal and mutant mice showed that the dependence of NMDA receptor channel conductance on voltage is not distinguishably different between normal and mutant mice (Fig. 4). The activation curves from both normal mice (n = 4) and mutant mice (n = 3) are well fitted by the equation developed by Jahr and Stevens [see legend to Fig. 4 (*20*)]. In summary, we could detect no differences between NMDA receptor function in normal and mutant mice.

Historic effects, as revealed by the response to the second of a stimulus pulse pair, did appear to be one aspect of synaptic function that differs between normal and mutant mice (Fig. 5). Although the slices from both normal and mutant mice showed paired pulse facilitation, the degree of facilitation was less in mutant mouse slices at all inter-pulse intervals tested. The impaired pulse facilitation in the mutant mice may not be surprising in that synapsin I, a molecule believed to be involved in making vesicles available for release, is regulated by CaMKII (*21*).

Deficient long-term potentiation. We have used two approaches to evaluate LTP in the mutant mice: field potential recording to survey properties of large populations of neurons, and whole cell recording to investigate LTP under conditions that are most sensitive for detecting the presence of LTP (the effect is typically larger with whole cell recordings than with field potentials), and to permit examination of the factors, such as the release probability, that participate in LTP.

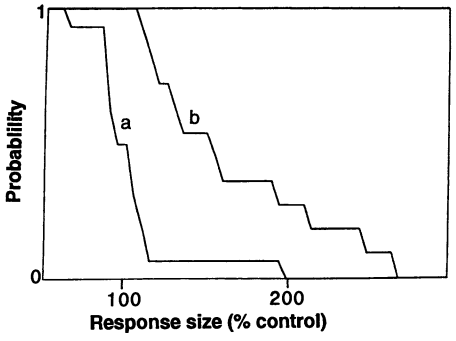

Fig. 7. Cumulative probability as a function of initial EPSP slope, expressed as percentage of the pre-tetanus average, and valued for neurons 30 to 60 minutes after tetanic stimulation. The 16 mutant slices are represented by plot a and 11 normal slices by plot b. The ordinate gives the fraction of the slices that exhibited a post-tetanic field EPSP slope of the corresponding abscissa size or smaller.

Fig. 8. Peak amplitude of synaptic current (EPSC) from whole cell recordings as a function of time. Amplitudes are expressed as a percentage of the mean amplitude before tetanic stimulation. (**A**) presents the data from a typical normal cell, (**B**) from a typical mutant cell, and (**C**) from one of two mutant cells that exhibited LTP. The sample traces labeled a and b in the graph show typical recordings of synaptic current made at the times indicated by the same letters in the amplitude graphs immediately below. The last of the three synaptic current traces is the preceding pair superimposed. Testing stimuli were given once each 2 s, and the points plotted here are averages of five consecutive samples. Holding potential was kept at either −60 or −70 mV (−60 mV for these data). The tetanus was given at the time point indicated by arrow head. The tetanus protocol was typically 50 Hz, 2 to 3 trains, 30 pulses for each train, and 10 to 11 s between trains while holding membrane potential at −30 to −40 mV (We observed that, with higher frequency tetani, such as 100 Hz, the synaptic current was often depressed, particularly in the mutant neurons.) The amplitude calibration bar (vertical) is 20 pA, and the time calibration bar (horizontal) is 10 ms. In many cases (including field potential recording), different things were tested between the time of data collection for synaptic strength; this accounts for the gaps in the graphs. In addition, two to seven different tetanus protocols were tested in some mutant neurons when the typical tetanus protocol did not induce LTP. These procedures made it difficult to average plots among neurons or slices in a precise way. Therefore, representative plots are shown.

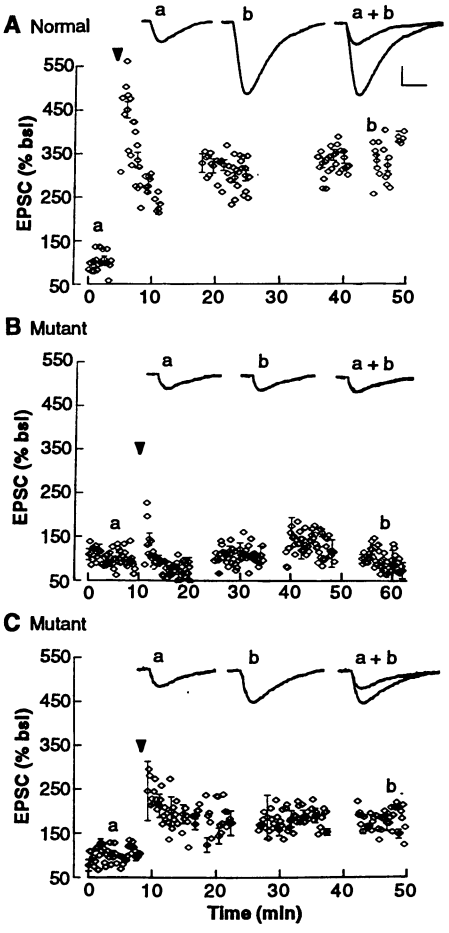

Table 1. Summary of the changes of synaptic strength in normal and mutant mice. n represents the number of slices (field EPSP slope) or neurons (EPSC amplitude).

Mouse	LTP n/ total n	Potentiation (% baseline)*	No LTP n/ total n	Change (% baseline)*
		Field EPSP		
Normal	9/11	183 ± 18	2/11	114 ± 1
Homozygote	2/16	168 ± 32	14/16	99 ± 3
Heterozygote	1/2	141	1/2	115
		EPSC		
Normal	9/10	286 ± 48	1/10	96
Homozygote	2/12	221 ± 39	10/12	98 ± 8

*Mean ± SEM.

The time course of synaptic strength in a normal and a mutant mouse after tetanic stimulation that typically induces LTP is shown in Fig. 6. In the normal mouse, the synaptic strength was obviously increased, but in the mutant mouse it was unchanged except for a usual amount of post-tetanic potentiation. Hippocampal slices from normal mice (9 of 11) exhibited LTP (defined as an increase in synaptic strength of 20 percent or greater, sustained for at least 30 minutes), whereas slices from only 2 of 16 mutant mice showed LTP (Table 1). The distribution of synaptic strength 30 to 60 minutes after a tetanus for 11 normal and 16 mutant neurons is shown in Fig. 7. Many mutant neurons actually showed some decrease in synaptic post-tetanus period. The effect was not just an increased threshold for LTP because, in slices from mutant mice, a second tetanus with increased trains (group of pulses, as indicated in legends of Figs. 6 and 8) still failed to produce potentiation. On the basis of field potential recordings that report the characteristics of large neuronal populations, we conclude that most hippocampal synapses do not exhibit significant LTP in mice lacking α-CaMKII.

During whole cell recording, nine of ten neurons from normal mice exhibited LTP with an average increase in synaptic strength of 286 percent (±48) of baseline at 30 to 60 minutes after a tetanic stimulus. For the mutant mice, 2 of 12 cells exhibited LTP, and the average synaptic strength after tetanic stimulation for these two cells was 221 percent (±34); for the neurons from mutant mice that did not show LTP (less than 20 percent increase) the average was 98 percent (±8, $n = 10$) (Table 1 and Fig. 8).

For normal cells, LTP is accompanied by a decrease in the number of "failures"—those stimuli that produce no postsynaptic response—and an increase in the quantal content as revealed by a standard quantal analysis (*22*). The synapses from one mutant animal that did exhibit LTP exhibit the same properties: a decrease in failures following tetanic stimulation (from a pre-tetanic failure rate of 2.3 percent to a post-tetanic rate of less than 0.07 percent) and an increase in quantal content that can account for the entire amount of potentiation.

We conclude, then, that mice lacking expression of α-CaMKII are markedly deficient in LTP, but in those cases where LTP does occur, it appears to be indistinguishable from what is observed in normal animals.

The mutant mice described above offer an interesting possibility for behavioral studies in that they show essentially normal postsynaptic function but deficient LTP. Our observations may also support earlier conclusions based on pharmacological experiments that CaMKII holoenzyme is involved in LTP (*9*), although this earlier work could not, of course, identify the α form as being involved. Because LTP was greatly diminished but apparently normal when present in the mutant mice, we think that α-CaMKII may be involved in a regulatory pathway for the processes responsible for LTP. Therefore, the magnitude of potentiation would be altered in the mutants, but any LTP that appeared would have usual characteristics. We cannot rule out the possibility that α-CaMKII is directly in the pathway for the production of LTP and that some other kinase (β-CaMKII, for example) is substituting in the instances where mutant mice exhibited LTP.

A deficit in LTP could be caused by a decreased number of connections between CA3 and CA1 neurons in the mutant mice. Although we have no anatomical evidence relating to number of connections, our electrophysiological data make this possibility highly unlikely. (i) Comparable stimulus intensities in normal and mutant mice produced comparable sized responses. (ii) The total depolarization for normal and mutant preparations was similar because the sizes of the responses were the same for both. (iii) For the whole cell experiments, we did not rely on synaptic depolarization for unblocking NMDA receptors at activated synapses; rather the cells, which were voltage-clamped, were held at membrane potentials of −30 or −40 mV during the tetanus, voltages that produce LTP even for exceedingly small inputs.

Although the precise role of α-CaMKII in LTP induction remains unknown, our α-CaMKII mutant mice should be useful in the identification of this role. We have tested the effect of α-CaMKII on the activities of protein kinase C (PKC), a kinase that has also been implicated in LTP induction (*9*). We found that the activity of PKC is normal in homogenates from the forebrains of mutant mice, suggesting that the targets of α-CaMKII are elsewhere. Synapsin I was shown to be one target for this kinase (*23*) and our observation of diminished paired pulse facilitation raises the possibility that the effect might be a presynaptic one. We also tested the hypothesis that α-CaMKII has the capacity to target the CaMKII holoenzyme to the membrane (*5*) where it can respond to localized increases in Ca^{2+} (*24*). We found that the proportion of the CaMKII holoenzyme activity associated with the membrane is unaltered in the forebrain of the mutant mice, which does not support the hypothesis (*25*).

The most remarkable feature of the α-CaMKII mutant mice is the apparent lack of widespread abnormality. The mice function, in the rather impoverished laboratory environment, like normal mice, and no gross neuroanatomical abnormality has been revealed in hippocampus and neocortex, two structures where α-CaMKII is particularly enriched. As demonstrated (*10*), however, the mutant mice are impaired in spatial-learning, which is thought to be based on hippocampal function (*2*). Likewise, a high-resolution analysis may very well reveal fine anatomical differences between the mutant mice and the wild-type control. At the electrophysiological level we have thus far analyzed only the hippocampal CA1 field cells. In light of the known distribution of α-CaMKII, cells in the other fields of the hippocampus, as well as in amygdala and the neocortex, should be examined for possible deficit. In this regard, LTP in the amygdala may be particularly worth examining; our α-CaMKII mutant mice seem to have an abnormally enhanced acoustic startle response, and LTP in the amygdala might be involved in the modulation of this response (*26*). Hence, this enhanced response might be another facet of the mutant mouse's deficit in LTP. The components of LTP are also thought to be involved in kindling, an animal model for epilepsy. Consequently, our mutant mice might also be useful for the study of the relation between LTP and kindling.

We view our results as a promising start in the application of the gene targeting technique (*3*) for the study of mammalian learning and memory. We have shown that interesting mutations can indeed have quite selective effects on neuronal processes, and we have produced a strain of mutant mice that should be useful for detailed behavioral studies.

REFERENCES AND NOTES

1. T. V. P. Bliss and T. J. Lomo, *J. Physiol.* **232**, 331 (1973).
2. R. G. M. Morris, S. Davis, S. P. Butcher, in *Long-Term Potentiation: A Debate of Current Issue*, M. Baudry and J. L. Davis, Eds. (MIT Press, Cambridge, 1991).
3. M. R. Capecchi, *Science* **244**, 1288 (1989).
4. H. Schulman and L. L. Lou, *Trends Biochem. Sci.* **14**, 62 (1989).
5. N. E. Erondu, M. B. Kennedy, *J. Neurosci.* **5**, 3270 (1985).
6. S. G. Miller, B. L. Patton, M. B. Kennedy, *Neuron* **1**, 593 (1988); P. I. Hanson *et al.*, *ibid.* **3**, 59 (1989).
7. S. G. Miller and M. B. Kennedy, *Cell* **44**, 861 (1986); J. E. Lisman and M. A. Goldring, *Proc. Natl. Acad. Sci. U.S.A.* **85**, 5320 (1988).
8. R. C. Malenka *et al.*, *Nature* **340**, 554 (1989).
9. R. Malinow, H. Schulman, R. W. Tsien, *Science* **245**, 862 (1989).
10. A. J. Silva, R. Paylor, J. M. Wehner, S. Tonegawa, *ibid.* **257**, 209 (1992).
11. C. N Adra *et al.*, *Cell* **60**, 65 (1987).
12. R. J. Colbran *et al.*, *Biochem. J.* **258**, 313 (1989).
13. S. Thompson, A. R. Clarke, A. M. Pow, M. L. Hooper, D. W. Melton, *Cell* **56**, 313 (1989).
14. The brain was isolated quickly, dissected, weighed and homogenized gently in four volumes of cold extraction buffer containing 10 mM tris-HCl (pH 7.4), 1 mM EGTA, 0.5 mM DTT, 0.1 mM PMSF (20 mg/liter), leupeptin (5 mg/liter), Soybean trypsin inhibitor (20 mg/liter). This homogenate was

kept on ice, and it was typically diluted 1/10 to 1/200 in the same cold buffer. The assays were carried out after 2- to 20-fold dilution of the homogenate in cold water, and immediately followed by the addition of cold assay buffer to a final concentration of 50 μM Syntide 2, 25 mM Hepes (pH 7.4), 10 mM MgCl, 0.5 mM DTT, 15 μM ATP and [γ-^{32}P]ATP at 50 μCi/ml. For the Ca^{2+}-CaM induced assays, we also added to this buffer 1.5 μM calmodulin and 2.0 mM $CaCl_2$. For the Ca^{2+}-CaM independent reactions, we added 0.5 mM EGTA to the assay buffer. After adding the assay buffer, reactions were briefly mixed and quickly placed at 30°C for 45 s. The reaction was terminated by spotting half of the reaction volume (25 μl) in perforated disks of phosphocellulose. These disks were then washed of nonincorporated [γ-^{32}P]ATP with 1 percent phosphoric acid and water. The radioactivity bound to the disks was counted and the values plotted. The phosphorylation results shown were derived from four independent experiments, each with at least three different concentrations of homogenates to check that substrate was not limiting, and with duplicates at each concentration point.

15. K. E. Burgin *et al.*, *J. Neurosci.* **10**, 1788 (1990).
16. We used 50 μM of peptide CaMKII272-302 described in reference 9.
17. R. J. Douglas, *Psychol. Bull.* **67**, 416 (1967).
18. All animal handling and tissue preparation were in accordance with a protocol approved by the Salk Institute and MIT Animal Use and Care Committee. Transverse hippocampal slices (~350 Im) were prepared from normal (wild) or mutant mice (male or female, 1 to 4.5 months old, mostly 1.5 to 3 months old). Slices were then maintained in an incubation chamber for at least 1 hour at room temperature (24° ± 1°C). An individual slice was transferred to a submerge–recording chamber where it was held by a net made with flattened platinum wire and nylon threads and continuously perfused with artificial cerebrospinal fluid (ACSF) at a rate of ~2 ml/min. The temperature in the recording chamber was 30.5° ± 0.5°C. The ACSF, equilibrated with 95 percent O_2 and 5 percent CO_2, is composed of (mM): NaCl (120), KCl (3.5), NaH_2PO_4 (1.25), $NaHCO_3$ (26), $MgCl_2$ (1.3), $CaCl_2$ (2.5), PCTX (0.05). The solution for dissection has the same composition as regular ACSF except there is no PCTX and NaCl is replaced with equimolar amounts of sucrose [G. K. Aghajanian and K. Rasmussen, *Synapse* **3**, 331 (1989)]. The CA3 region was usually removed to prevent epileptiform activity. The cell layer was visualized under an inverted microscope with phase contrast (Zeiss). Extracellular field excitatory postsynaptic potentials (f-EPSP's) were recorded in the stratum radiatum of CA1 with electrodes (1 to 2 Mohm) filled with ACSF. Excitatory post-synaptic currents (EPSC's) were recorded in CA1 pyramidal neurons with the whole-cell patch-clamp mode; electrodes (3 to 4 Mohm); no fire polishing; soft glass (Drummond) filled with (mM) cesium gluconate (130), $CsCl_2$ (5), EGTA (0.5), $MgCl_2$ (1), Mg-ATP (2), GTP (0.2), NaCl (5), Hepes (10); pH 7.25. The seal formed on cell bodies was typically 2 to 3 Gohm and the input resistance of cells was typically around 100 Mohm. The Bipolar tungsten stimulating electrodes (Frederick Haer & Co.) were positioned in Schaffer collateral-commissural afferents to evoke f-EPSP's (150 to 200 μm away) or evoke EPSC's (50 to 100 μm away). The stimulus intensity was adjusted to evoke pretetanic responses of similar sizes for all the neurons or slices. The stimulus duration was 100 μs. Recordings were performed with an Axopatch-1A (Axon Instruments, Inc.), filtered at 1 to 2 kHz, and sampled at 5 to 10 kHz. Data were collected and analyzed with programs written by C. F. Stevens in AxoBASIC/QuickBASIC. The data collected from normal other strain of mice were combined with the data from normal littermates, since they were indistinguishable. CNQX and D-APV (D-2-amino-5-phosphonovaleric acid) were from Cambridge Research Biochemicals and PCTX was from Sigma.
19. L. Chen and L. Y. M. Huang, *Nature* **356**, 521 (1992).
20. C. E. Jahr and C. F. Stevens, *J. Neurosci.* **10**, 1830 (1990); *ibid.*, p. 3178.
21. J. W. Lin *et al.*, *Proc. Natl. Acad. Sci. U.S.A.* **87**, 8257 (1990).
22. J. M. Bekkers and C. F. Stevens, *Nature* **346**, 724 (1990); R. Malinow and R. W. Tsien, *ibid.*, p. 177.
23. T. McGuiness, Y. Lai, P. Greengard, *J. Biol. Chem.* **260**, 1969 (1985).
24. W. Muller, J. A. Connor, *Nature* **354**, 74 (1991); P. B. Guthrie, M. Segal, S. B. Kater, *ibid.*, p. 76.
25. A. J. Silva, unpublished data.
26. W. A. Falls, M. J. D. Miserendino, M. Davis, *J. Neurosci.* **12**, 854 (1992); M. Davis, *Tips* **13**, 35 (1992).
27. The 6.1-kb genomic fragment present in p23 was obtained after Pvu II digestion of cosmid 14.4. This cosmid was cloned from a C57B1/6J library with a Sph I–Pvu II fragment from an α-CaMKII full-length cDNA that only detects α-CaMKII. The *neo* gene was inserted within the 6.1-kb genomic-fragment at the deleted 130 bp Sph I fragment, and its transcriptional orientation, is the same as the endogenous α-CaMKII.
28. The DNA samples (5 μg) shown in the autoradiograph were digested with Pvu II restriction enzyme, blotted to nylon membranes, and probed with radioactively labeled p23 (1 × 10^9 cpm/μg). We used only mutation homozygotes that were F1 progeny from crosses between these mutant heterozygous.
29. We have also analyzed the Western blots shown with a polyclonal antibody that recognizes α- and β-CaMKII. This antibody has a wider specificity, and it might have recognized any other proteins resulting from the fusion between α-CaMKII and the inserted *neo*.

30. We thank A. Smith, Y. Ichikawa, M. B. Kennedy, M. Hooper, N. Waxman, and P. Kelly for advice or various invaluable reagents (or both); J. R. Pauly, G. Schneider, and R. Erzurumlu for help with the neuroanatomy. Supported by Howard Hughes Medical Institute (S.T. and C.F.S.), Human Frontier Science Program grant #76834 (S.T.), and NIH grant 5 R01 NS 12961-17 (C.F.S.).

10 June 1992; accepted 19 June 1992

Impaired Spatial Learning in α-Calcium-Calmodulin Kinase II Mutant Mice

Alcino J. Silva, Richard Paylor, Jeanne M. Wehner, Susumu Tonegawa

Although long-term potentiation (LTP) has been studied as the mechanism for hippocampus-dependent learning and memory, evidence for this hypothesis is still incomplete. The mice with a mutation in the α-calcium-calmodulin–dependent kinase II (α-CaMKII), a synaptic protein enriched in the hippocampus, are appropriate for addressing this issue because the hippocampus of these mice is deficient in LTP but maintains intact postsynaptic mechanisms. These mutant mice exhibit specific learning impairments, an indication that α-CaMKII has a prominent role in spatial learning, but that it is not essential for some types of non-spatial learning. The data considerably strengthen the contention that the synaptic changes exhibited in LTP are the basis for spatial memory.

Changes in synaptic strength may be critical for learning either as a mechanism for the direct storage of memories, or as a process that transforms information making it suitable for long-term storage (*1*). Long-term potential (LTP) is a stable and long-lasting potentiation of synaptic activity which follows Hebbian rules (*2*). Hence, it is widely thought that LTP is a physiological mechanism underlying learning and memory processes. The *N*-methyl-D-aspartate receptor (NMDAR) is a voltage-sensitive and glutamate-gated channel, and it regulates a calcium current essential for the induction of LTP (*3*). The evidence supporting the linkage between LTP and mammalian learning and memory primarily comes from the analysis of rats in which the NMDAR was blocked by the antagonist, aminophosphonovaleric acid (APV) (*4*). The interpretation of those results is difficult because inhibiting NMDAR function also disrupts synaptic function (*5*) and therefore might alter the character of information processing in the hippocampus. Thus, the deficits in learning could be due to this alteration in hippocampal synaptic function, and not to the deficits in LTP. A second line of evidence linking LTP to learning and memory comes from electrophysiological experiments that show that induction of saturating levels of LTP in the hippocampus impairs the ability of rats to acquire new spatial information (*6*). However, these findings have also been alternatively interpreted (*7*).

It is thus important to develop addition-

A. J. Silva and S. Tonegawa are at the Howard Hughes Medical Institute, Center for Cancer Research and Department of Biology, Massachusetts Institute of Technology, Cambridge, MA 02139.
R. Paylor and J. M. Wehner are at the Institute for Behavioral Genetics, University of Colorado, Boulder, CO 80309.